EFDA–JET–PR(10)65

J. Hobirk, F. Imbeaux, F. Crisanti, P. Buratti, C.D. Challis, E. Joffrin, B. Alper, Y. Andrew, P. Beaumont, M. Beurskens, A. Boboc, A. Botrugno, M. Brix, G. Calabro', I. Coffey, S. Conroy, O. Ford, D. Frigione, J. Garcia, C. Giroud, N.C. Hawkes, D. Howell, I. Jenkins, D. Keeling, M. Kempenaars, H. Leggate, P. Lotte, E. de la Luna, G. P.Maddison, P.Mantica, C. Mazzotta, D.C. McDonald, A. Meigs, I. Nunes, E. Rachlew, F. Rimini, M. Schneider, A.C.C. Sips, J.K. Stober, W. Studholme, T. Tala, M. Tsalas, I. Voitsekhovitch, P.C. de Vries and JET EFDA contributors

Improved Confinement in JET Hybrid Discharges

Improved Confinement in JET Hybrid Discharges

J. Hobirk[1], F. Imbeaux[2], F. Crisanti[3], P. Buratti[3], C.D. Challis[4], E. Joffrin[2,5], B. Alper[4], Y. Andrew[4], P. Beaumont[4], M. Beurskens[4], A. Boboc[4], A. Botrugno[3], M. Brix[4], G. Calabro'[3], I. Coffey[6], S. Conroy[7], O. Ford[4], D. Frigione[3], J. Garcia[2], C. Giroud[4], N.C. Hawkes[4], D. Howell[4], I. Jenkins[4], D. Keeling[4], M. Kempenaars[4], H. Leggate[4], P. Lotte[2], E. de la Luna[5], G. P.Maddison[4], P. Mantica[8], C. Mazzotta[3], D.C. McDonald[4], A. Meigs[4], I. Nunes[9], E. Rachlew[10], F. Rimini[5], M. Schneider[2], A.C.C. Sips[5], J.K. Stober[1], W. Studholme[4], T. Tala[11], M. Tsalas[12], I. Voitsekhovitch[4], P.C. de Vries[12] and JET EFDA contributors*

JET-EFDA, Culham Science Centre, OX14 3DB, Abingdon, UK

[1]Max-Planck-Institut für Plasmaphysik, EURATOM Association, Boltzmannstr. 2, 85748 Garching
[2]CEA, IRFM, F-13108 Saint-Paul-lez-Durance, France
[3]ASSOCIAZIONE EURATOM-ENEA sulla Fusione C.R. FRASCATI, CP65, 00044 Frascati - Italy
[4]EURATOM-CCFE Fusion Association, Culham Science Centre, OX14 3DB, Abingdon, OXON, UK
[5]EFDA CSU Culham, Culham Science Centre, OX14 3DB, Abingdon, OXON, UK
[6]Queen's University, Belfast, BT7 1NN, UK
[7]Association Euratom, Dept. Physics and Astronomy, Uppsala University, SE 75121 Uppsala
[8]Instituto di Fisica del Plasma, Associazone EURATOM ENEA -CNR, Milano, Italy
[9]Instituto de Plasmas e Fuso Nuclear, Associao EURATOM-IST, 1049-001 Lisboa, Portugal
[10]Association Euratom-VR, Dept. Phys., KTH. SE 10691, Stockholm Sweden
[11]Association Euratom-Tekes, VTT, P.O. Box 1000, 02044 VTT, Finland
[12]FOMinstitute Rijnhuizen, EURATOMassociation, P.O. Box 1207, 3430BE, Nieuwegein, Netherlands
** See annex of F. Romanelli et al, "Overview of JET Results",*
(23rd IAEA Fusion Energy Conference, Daejon, Republic of Korea (2010)).

Preprint of Paper to be submitted for publication in
Plasma Physics and Controlled Fusion

ABSTRACT

A new technique has been developed to produce plasmas with improved confinement relative to the $H_{98,y2}$ scaling law on the JET Tokamak. In the mid size Tokamaks ASDEX Upgrade and DIII-D heating during the current formation is used to produce a flat q-profile with a minimum close to 1. On JET this technique leads to q-profiles with similar minimum q but opposite to the other Tokamaks not to an improved confinement state. By changing the method utilising a faster current ramp with temporary higher current than in the flattop (current over shoot) plasmas with improved confinement ($H_{98,y2} = 1.35$) and good stability (bN Section 1 3) have been produced and extended to many confinement times only limited by technical constraints. This paper will introduce the q-profile forming method, the consequent current diffusion and will discuss the effect on the kinetic profiles in phases without the presence of Neo-classical Tearing Modes (NTMs).

INTRODUCTION

Over the past 10 years a new scenario has emerged on the mid-size tokamaks ASDEX Upgrade [1, 2, 3] and DIII-D [4, 5] which combines a higher q_{95} operation with improved confinement compared to the $H_{98,y2}$ scaling law called hybrid scenario or improved H-mode. Could this kind of scenario be reproduced on ITER, new possibilities would arise, e.g. high Q operation at reduced IP [6, 7]. Hybrid scenario plasmas can have significantly improved confinement above the standard H98,y2 H-mode scaling but the physics basis remains somewhat unclear. At JET [8] discharges similar to the ones from DIII-D and ASDEX Upgrade have been carried out in a high triangularity configuration before the 2008/9 campaigns. The q-profile modification has been done with low power (0.5-1.2MW) Lower Hybrid Current Drive (LHCD). Careful analysis later has shown that the initial q-profile modification was lost quite rapidly and well before the high power/high beta phase at the end of the additional heating phase. The discharges were done at low current and high (normalised) density. Nevertheless some of the characteristics e.g. the stability against Neoclassical Tearing Modes (NTM) have been reproduced but the confinement was not improved significantly over the $H_{98,y2}$ scaling.

New experiments in JET in a low triangularity configuration with low plasma densities have been done to explore the differences between the JET discharges ($H_{98,y2} = 1$) to discharges from other experiments $1 < H_{98,y2} < 1.8$. The configuration has been chosen such that the results can be compared to earlier JET pulses [9] and to pulses from ASDEX Upgrade. Further more the low plasma density expected from H-mode discharges in this low triangularity configuration results in higher temperatures and longer current diffusion time scales so that possible transient effects can be better observed. The methods developed for the low triangularity configuration has later been ported to plasmas in a high triangularity configuration and higher density which has been reported in [10]. The experiment started from the assumption that the central part of the q-profile plays an important role for explaining the observed differences between the different tokamaks as shown as one reason on ASDEX Upgrade [11].

1. Q-PROFILE MODIFICATION

In the new experiments different experimental strategies to modify the central part of the q-profile have been tried. The first method utilised early NBI heating similarly as it is done on ASDEX Upgrade and DIII-D. Two different waveforms were tested, firstly a long NBI prelude with low power NBI (3-5MW) starting at t = 2s and secondly a short NBI prelude starting at t = 3–3.5s but with P_{NBI} =10MW. The P_{NBI} is increased to values of 16-22MWat the time of the current flattop at t = 4s. In both cases it was possible to delay the onset of sawteeth significantly and to flatten the central part of the q-profile. The normalised confinement did not change significantly. The next idea tried was to use Ion Cyclotron Heating in H-minority Regime (ICRH) at approximately half radius from t = 2s on. The main idea was to broaden the electron temperature profile and consequently the ohmic current profile which in the absence of external current drive is dominating the total current profile. Unfortunately the electron temperature profile shape did not change by much and only the higher temperature has let to a higher q at the start of the main heating but again not to changed confinement properties. The last method tested in this series was to change the current ramp rate without applying additional heating. The introduced current density is located at the edge and needs to diffuse inwards for several seconds before it reaches the centre. Therefore if the current is risen fast then transiently more current is outside the plasma core and the current density profile is broader. In some of those pulses an increased confinement up to $H_{98,y2} = 1.1$ has been observed but is still not as good as on other experiments.

Analysis with the transport code TRANSP [12] have indicated that all these methods do not produce a q-profile which is as broad as on ASDEX Upgrade measured by the radius of the q = 1.5 surface as seen as 3/2 NTMposition [11]. The current density profile produced by the faster current ramp is already relatively flat and it seemed not to be possible to extend the low shear region by just redistributing central current densities. As a result of this consideration a current ramp down after a short plateau was introduced (a current “overshoot”) to mobilise current from the outer part of the plasma and to change the outer part of the q-profile (see figure 1 with the plasma current trace in black).

2. IMPROVED CONFINEMENT REACHED

Improved confinement up to $H_{98,y2} = 1.4$ has been reached transiently by modification of the qprofile consisting of a further flattening of the q-profile in the core and a reduction of the current density in the outer third of the plasma. Using this strategy the q-profile can be influenced by the initial current ramp rate, the length of the first plateau of the current over shoot and the ramp down rate. The target q_0 is strongly connected to the start time of the heating. By such modifications to the q-profile the MHD stability and the improved performance could be extended to about 5s duration. This was only limited by technical constrains due a temperature limit in the NBI duct. In figure 1 some of the characteristic data of such a pulse (Pulse No: 75225) in comparison to a pulse without strong q-profile modification (Pulse No: 74826) are shown. The dimensional parameters of discharges discussed can be found in table 1 and the dimensionless parameters in table 2. For those two pulses

the line averaged densities are similar, the same plasma shape is used and the NBI heating starts at the same time. Consequences of the change in target q-profile are different n-number NTMs in the plasma but also the global confinement as indicated by the $H_{98,y2}$ factor is different. In figure 2 the q-profile from EFIT constrained by MSE and pressure data (including fast ion pressure) at 2.45s after start of the heating is shown. The q-profile of Pulse No: 75225 has a large low shear region up to R = 3.4m compared to Pulse No: 74826. Also the positions of the critical rational q surfaces for NTM stability (as indicated in figure 2) are moved significantly outward in Pulse No: 75225. The density in Pulse No: 75225 is higher at t = 6s but relaxing later in the pulse to the same values as in Pulse No: 74826 at t = 5.6s . Many parameters in Pulse No: 74826 are dominated by the existence of the n = 2 NTM, in particular stored energy and plasma density. Therefore it is difficult to compare the time traces to the ones of Pulse No: 75225 where only a n = 3 NTM is active and only for a comparatively short time. As a consequence all the following profile comparison is done for an early time point which is NTM free in both discharges but might still be transient.

3. DIFFERENCES IN KINETIC PROFILES

The electron and ion temperature (see figure 3) in Pulse No: 75225 are higher for any radius and the electron density is higher as well for any radius compared to Pulse No: 74826. The differences in the kinetic pressure seen in figure 3 explain within 5% the difference in H-factor in table 2. The differences clearly start in the H-mode pedestal and are then propagated towards the centre as reported for ASDEX Upgrade improved H-mode [13]. The ion temperature profile is not constant during the pulse. Even the the ion temperature gradient length varies with time and radius therefore it is difficult to make a straight conclusion on changes of transport. The inverse gradient length and the Mach number are listed in table 2. The inverse gradient length is slightly higher for the pulse with lower normalised confinement but the Mach number is slightly lower. Unfortunately the profile changes shown by 3 are not always the case. In figure 4 profiles are shown for a pair of pulses done at 2MA/2.4T. Pulse No: 73306 has been done with some NBI preheat but without current overshoot($H_{98,y2} \approx 1$), the other Pulse No: 74836 has been done following the recipe developed at 1.7MA/2T with a current overshoot ($H_{98,y2} = 1.2$). The profiles are now such that the stored energy in the core is constant and the whole difference can be attributed to a change in edge stored energy (see table 1). $W_{pedestal}$ is determined by integrating the pressure profile outside the $\Psi_{pedestal}$ and taking the value of the pressure at $\Psi_{pedestal}$ constant inside. $\Psi_{pedestal}$ is defined here as the poloidal flux where the derivative of the pressure becomes smallest within $\Psi \geq 0.8$. The result has been inspected visually and represents the pedestal top reasonably well. Only in the later discussed cases (Pulse No: 75625-7) with pressure profiles build with the help of LIDAR data the $\Psi_{pedestal}$ becomes uncertain because the spatial resolution is not sufficient. In figure 6 profiles from another comparison pair at 1.7MA/2T are shown. In this case Pulse No: 79630 has been done without current overshoot and significantly delayed NBI injection to produce a q-profile as close as possible to fully diffused H-mode qprofile. Nevertheless the confinement time is still larger than the scaling predicts ($H_{98,y2} = 1.2$)the reason for this is not clear. Several parameters are different than in the normally

performed H-mode discharges, firstly the normalised beta is higher ($\beta_N = 2.7$), secondly the density and consequently the collisionality is lower and last but not least the q-profile is still different due to the early heating. This is a necessity because the plasma shape is relatively l_i sensitive and would touch the wall if run with L-mode l_i-values. The achieved q-profile is a compromise between maintaining the chosen shape and relaxing it fully. The list of parameters stated here is most likely not complete and it is not yet possible to say which parameter might be the key in understanding the difference of the achieved confinement time to the scaled confinement time. The comparison Pulse No: 79628 has been done at the same plasma parameters as the earlier discussed Pulse No: 75225 ($H_{98,y2} = 1.35$,see also table 1). In this case the edge stored energy is the same for both pulses and the additional energy can be found in the plasma core. A possible mechanism is discussed in [14] based on the idea that the high rotation speed together with low magnetic shear in the core can influence the turbulence properties and can reduce the ion temperature stiffness. The three cases presented show the difficulty to determine from which part of the profile the improved confinement comes from. The total energy is most often changed by about 20-30% and several profiles can be different. Therefore it is difficult to pin down the changes in stored energy to certain profile effects. Nevertheless, in the cases with highest confinement the pedestal and the core profiles seem to be improved. But in other cases a pedestal improvement or a core improvement can be found. Up to now no criteria has been found to determine when the different improvements take place because the different discharges seem to be rather similar and the changes are often too small to make a strong conclusion.

4. POWER SCALING

Another observation is that in this kind of pulses the normalised confinement increases with increasing input power, or in other words the power degradation in the $H_{98,y2}$ scaling law is too negative. This has been observed e.g. on ASDEX Upgrade [7], DIII-D [15] and JET [16]. On the other hand in dedicated experiments it was also found that the $H_{98,y2}$ scaling law fits reasonably well [17]. The papers cited above use different data bases and include partially H-modes without active q-profile forming. In figure 7 the confinement properties of 3 different pulses are shown. The highest power pulse has been done at the same plasma parameters as the earlier example Pulse No: 75225 (See also table 1). The other two pulses are a beta scan (the neutral beam injected power is feedback controlled on the measured diamagnetic poloidal beta) at similar plasma parameters, e.g. electron densities (feedback controlled but with very similar gas flow) and plasma shaping. The lowest power pulse exhibits a normalised confinement a little better than the scaling, the medium power case has a significant improved normalised confinement and the highest power has the best normalised confinement. Even though the experiment has been carried out as beta scan it is not easy to make a conclusion on the beta scaling because e.g. the normalised gyro radius $\rho*$ is changing as well in this scan. Also the rotation speed does vary largely (similar to the ion temperature, see also table 1) due to the difference in NBI heating but the Mach number is similar. In figure 8 the kinetic profiles of the three different pulses for $t = 7.5$s are shown. The line averaged electron density (See

table 1) has been kept constant but a small tendency to peak centrally with increasing NBI power and fuelling is visible. It can also be seen that the gain in stored energy is mostly in the ion channel (as it has been seen on ASDEX Upgrade [18]). The increased heating power is mainly coupled to the ions for the beam energy used. The low densities lead to a weak coupling of the ions to the electrons, therefore this change of T_i/T_e was almost expected. In the comparison of those pulses the heating power is not constant in this case the (ion-) temperature pedestal is increasing significantly. Using the shown kinetic profiles and calculating the pedestal contribution to the total kinetic stored energy the contribution is about 30% with large error bars. The calculated number for the low heating power discharge is slightly larger and amounts to 33%. The inverse ion temperature gradient length is increasing from the lowest to the highest power pulse.

5. Q-PROFILE DEVELOPMENT

In the following four different q-profile time developments will be discussed. Firstly a EFIT calculation with MSE data and pressure profile constraints using a spline representation for the poloidal flux function (will be called in short MSE q). Secondly a EFIT calculation with Faraday rotation and interferometric density input without pressure constraint and using low order polynomials as representation for the poloidal flux function (in short FR q). There are some systematic differences between the FR q-profiles and the MSE q-profiles. Those differences reflect partially the uncertainties in the q-profile reconstruction in the sense that firstly the pressure constraint is missing, secondly the reconstructed electron density profile within EFIT is not showing the full details because only 4 chords are used and thirdly due to the availability of only 5 chords of the Faraday rotation measurement a low order polynomial is used to represent the poloidal flux function. These effects make in this paper a FR q-profile less reliable than the MSE q-profile. On the other hand, due to the late heating the MSE diagnostic is not available before t = 5.26s and the trend in the q profile is quite consistent independent of the diagnostic except in the very core for a limited amount of time.

The third an fourth q-profiles were calculated by the TRANSP code using experimental data from HRTS (n_e,T_e) and charge exchange diagnostic (T_i,Z_{eff}) as input and using neoclassical resistivity and a neutral beam current drive model as basis [12]. The difference between the two calculations is the starting q-profile which is a FR q at t = 3s in one case and a MSE q at t = 5.26s in the other case. The fifth q-profile was calculated by the transport code CRONOS [19] starting with the MSE q and the same experimental profiles as used in TRANSP.

In the discussed plasma the confinement improvement appears to be triggered if not caused by a modification of the outer part of the q-profile by utilising a current overshoot technique. Naturally the fast change of q will disappear on a similar time scale as introduced with a delay caused by the increased temperature due to the applied strong heating. The time traces in figure 5 show that indeed most of the change in the outer part of the q-profile has been removed by current diffusion after about 2s, however the confinement for Pulse No: 75225 remains high. There is some small trend left (especially in the core) for the rest of the heating period - the q-profile does not reach

an equilibrium during the heating period. Qualitatively the TRANSP and CRONOS calculations reproduce the trend and indicate that classical current diffusion may be sufficient to explain the changes in q within the measurement uncertainties. A similar analysis for a pulse without current over shoot e.g. Pulse No: 74826 is tainted by the occurrence of a low n-number NTM. Differences in q are being expected (as can be seen in figure 2) because the temperature and Zeff profiles are different (as can be seen in 3).

6. SUMMARY AND DISCUSSION

Experiments were performed on JET to scan the q-profile with a central q around 1 to see if a domain could be found where the confinement can be improved significantly compared to a H-mode with a non modified q-profile. Different methods have been tried to change the q-profile which mainly change the central part of the q-profile based on the assumption that a low shear in the centre allows the hybrid scenario to reach higher confinement. This approach was not successful on JET at first and a larger change in the core q-profile and a change in the outer part of the q-profile was necessary to improve the confinement significantly. On JET the chosen method up to now is a small current ramp down after a fast current ramp up and immediate strong heating following. The confinement improvement can affect the whole profile and is not localised. An improved pedestal pressure together with changed transport properties in the core lead to an enhanced confinement. The confinement enhancement survives the decay of the change in current profile in the outer part of the plasma by current diffusion by a significant amount of time in the low triangularity configuration. Calculations by TRANSP and CRONOS can follow the experimental q-profile evolution indicating that classical current diffusion may be enough to explain the q evolution. This scenario operates at high normalised beta and a main difficulty are NTMs. Furthermore, is has been shown that in this scenario the normalised confinement improves with higher applied power. A relatively stable regime has been reached at low triangularity with only 5/4 or 4/3 NTMs. Assuming that these plasmas have a close relationship to the ASDEX Upgrade and DIII-D hybrid plasma then the scenario has been shown to be extendable to lower $\rho*$, breaking the trend reported in [20] and hence showing potential to be ported to ITER. Remaining problems are mainly MHD related and may be less severe for ITER because of its ECCD capability allowing NTM stabilisation. However, many physics questions remain open including how the scenario can be used at higher densities, lower rotation speeds, with impurity seeding and whether continuous current drive would be necessary to maintain it.

ACKNOWLEDGEMENT

This work was supported by EURATOM and carried out within the framework of the European Fusion Development Agreement. The views and opinions expressed herein do not necessarily reflect those of the European Commission.

REFERENCES

[1]. O. Gruber et al., Physical Review Letters **83**, 1787 (1999).

[2]. R. Wolf et al., Plasma Physics and Controlled Fusion **41**, B93 (1999).
[3]. A. Staebler et al., Nuclear Fusion **45**, 617 (2005).
[4]. T.C. Luce et al., Nuclear Fusion **41**, 1585 (2001).
[5]. T.C. Luce et al., Physics of Plasmas **11**, 2627 (2004).
[6]. M.R. Wade et al., Nuclear Fusion **45**, 407 (2005).
[7]. A. Sips et al., Nuclear Fusion **47**, 1485 (2007).
[8]. E. Joffrin et al., Proceedings of the 22nd IAEA Fusion Energy Conference, Geneva, Switzerland (2008).
[9]. E. Joffrin et al., Nuclear Fusion **45**, 626 (2005).
[10]. E. Joffrin et al., Proceedings of the 23nd IAEA Fusion Energy Conference, Daejon, Republic of Korea (2010).
[11]. J. Stober et al., Nuclear Fusion **47**, 728 (2007).
[12]. R.V. Budny et al., Physics of Plasmas **7**, 5038 (2000).
[13]. C.F. Maggi et al., Nuclear Fusion **47**, 535 (2007).
[14]. P. Mantica et al., Proceedings of the 23nd IAEA Fusion Energy Conference, Daejon, Republic of Korea (2010).
[15]. C. Petty et al., Physics of Plasmas **11**, 2514 (2004).
[16]. D.C. McDonald et al., Plasma Physics and Controlled Fusion **46**, A215 (2004).
[17]. L. Vermare et al., Nuclear Fusion **47**, 490 (2007).
[18]. A. Manini et al., Nuclear Fusion **46**, 1047 (2006).
[19]. J.F. Artaud et al., Nuclear Fusion **50**, 043001 (2010).
[20]. D.C. McDonald et al., Plasma Physics and Controlled Fusion **50**, 124013 (2008).

Pulse No:	Time	I_P	B_T	$\bar{n}_e$	P_{NBI}	β_N^{tot}	W_{core}	W_{pedestal}	ω_{tor}
	[s]	[MA]	[T]	[$10^{19}\mathrm{m}^{-3}$]	[MW]		[MJ]	[MJ]	krad/s
75225	7.25	1.7	2	3.24	18.8	2.92	1.83	1.02	77.2
74826	7.25	1.7	2	3.12	19.2	2.52	1.68	0.8	65.3
75225	6 ± 0.2	1.7	2	3.6	18.8	3.07	1.98	1.02	76.7
74826	5.6 ± 0.1	1.7	2	3.35	19.2	2.58	1.65	0.83	55.5
79630	7 ± 0.2	1.7	2	3.56	17.5	2.55	1.64	0.98	77.8
79628	7 ± 0.2	1.7	2	3.2	17.5	2.83	1.85	1.07	82.4
73306	8.1 ± 0.2	2	2.4	3.51	20	2.21	2.24	0.93	79.8
74836	8.1 ± 0.2	2	2.4	3.9	22	2.63	2.32	1.29	75.7
75625	7.5 ± 0.2	1.7	2	3.1	17	2.8	2.2	0.79	86.2
75626	7.5 ± 0.2	1.7	2	3.1	9.4	1.8	1.32	0.69	53.8
75627	7.5 ± 0.2	1.7	2	3.0	13.5	2.26	1.89	0.44	66.4

Table 1: List of dimensional 0d parameters for all pulses and used times and average interval. Toroidal angular frequency measured at R=3.4m.

Pulse No:	Time [s]	$H_{98,y2}$	ρ* 10^{-3}	ν* 10^{-3}	β_N^{th}	q_{95}	R/L_{T_i}	M	MHD	CuOv
75225	7.25	1.27	5.87	12	1.96	3.94	6.2	0.47	n=3,FB	Yes
74826	7.25	0.98	5.32	19	1.52	3.77	6.3	0.42	n=2,n=3	No
75225	6 ± 0.2	1.29	5.69	12	2.16	3.96	6.6	0.49	-	Yes
74826	5.6 ± 0.1	1.02	5.34	20	1.65	3.77	7.3	0.4	n=1,n=3	No
79630	7 ± 0.2	1.16	5.48	18	1.88	3.87	6.4	0.52	FB,n=4	No
79628	7 ± 0.2	1.31	5.89	12	2	3.94	6	0.48	FB,n=5	Yes
73306	8.1 ± 0.2	1.09	5.09	13	1.53	3.8	6.5	0.47	n=3,n=5	No
74836	8.1 ± 0.2	1.22	5.13	13	1.81	3.95	6.5	0.43	FB,n=4,n=5	Yes
75625	7.5 ± 0.2	1.27	5.9	12	1.9	3.95	6.7	0.5	FB,n=4,n=5	Yes
75626	7.5 ± 0.2	1.07	4.93	23	1.32	3.77	5.6	0.45	n=1	Yes
75627	7.5 ± 0.2	1.14	5.45	15	1.56	3.84	6.3	0.48	FB,n=1,n=4	Yes

Table 2: List of non-dimensional 0d parameters for all pulses and used times and average interval. R/L_{Ti} and the Mach number (defined as $M = \sqrt{\frac{m}{e}}\frac{v}{\sqrt{T_i}}$ are measured at R = 3.4m.MHD information includes only core MHD and n=1 is also m=1, FB is the abbreviation for fishbones and Saw is the abbreviation for sawteeth. The label CuOv indicates whether the current overshoot technique was used in this pulse or not.

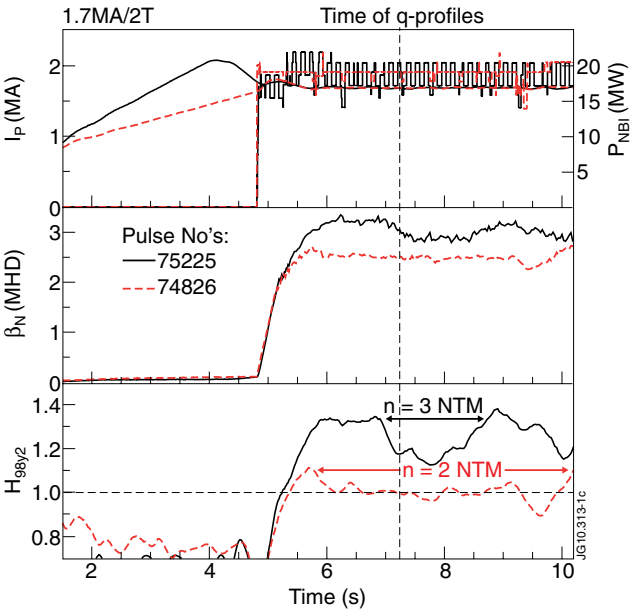

Figure 1: Time traces of a JET hybrid discharge with current ramp down before the main heating (current overshoot) in black compared to a pulse without strong q-profile modification in a dashed red line. In the upper graph the traces of the plasma current and the NBI heating power are shown. In the middle the normalised beta bN and in the lower graph the $H_{98,y2}$-factor is drawn.

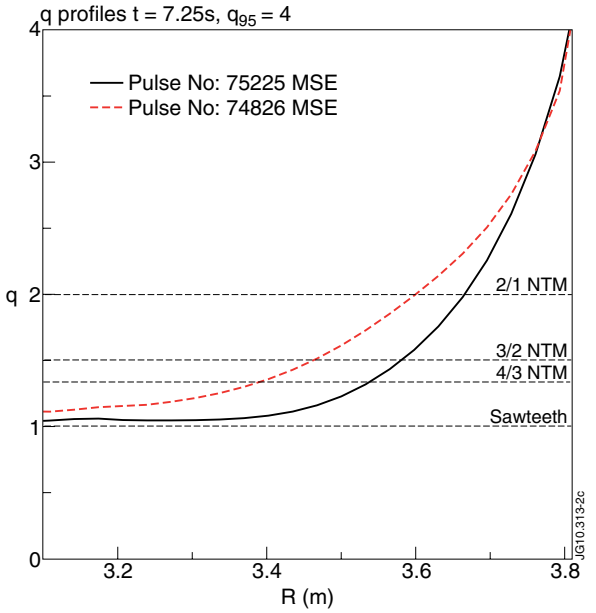

Figure 2: Equilibrium reconstructed q profile 2.45s after start of the main heating for a pulse with current overshoot in black and a pulse without in dashed red.

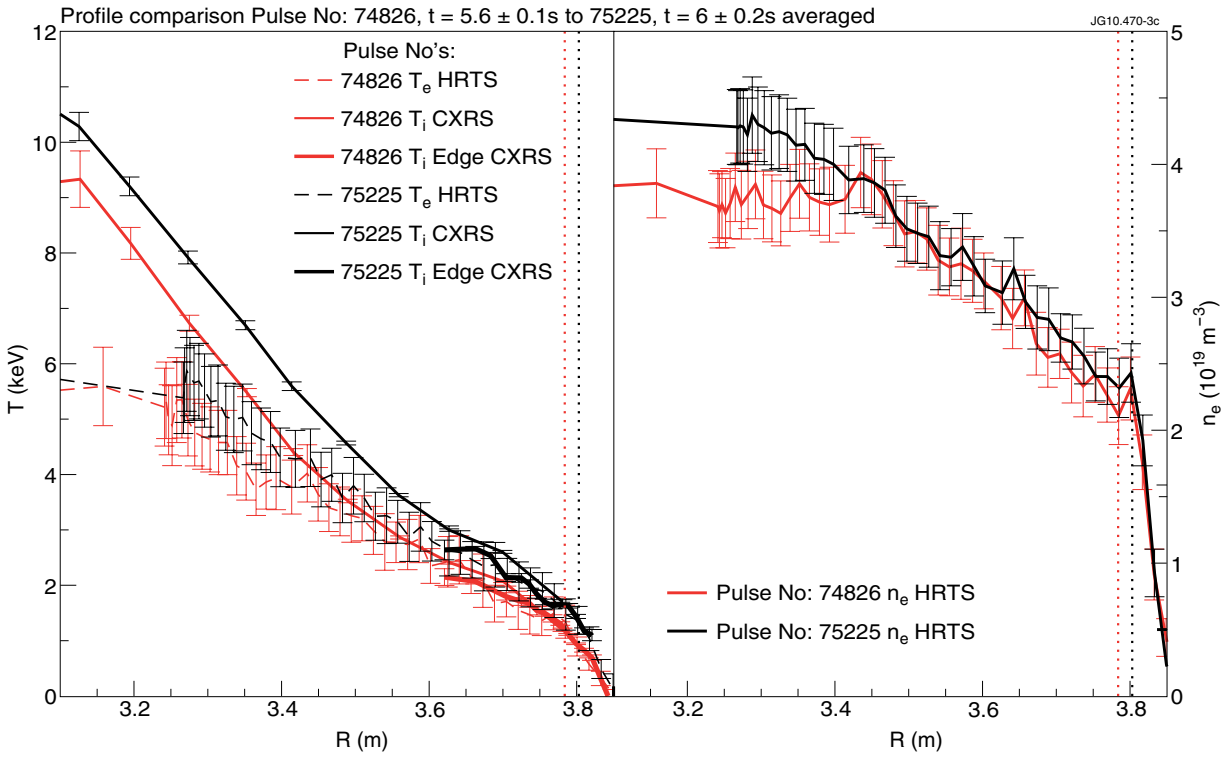

Figure 3: Temperature profiles from a pulse with modified q-profile in black (current overshoot) and without modified q-profile in red. The profile in closed lines are ion temperatures measured by Charge Exchange Recombination Spectroscopy (CXRS). Closed thick lines are from the edge CXRS system. Dashed lines are electron temperatures measured by the High Resolution Thomson Scattering (HRTS) diagnostic. On the right hand side the corresponding density profiles from HRTS. The pedestal radius used to derive the pedestal energy for table 1 is indicated as dotted line in the appropriate colour.

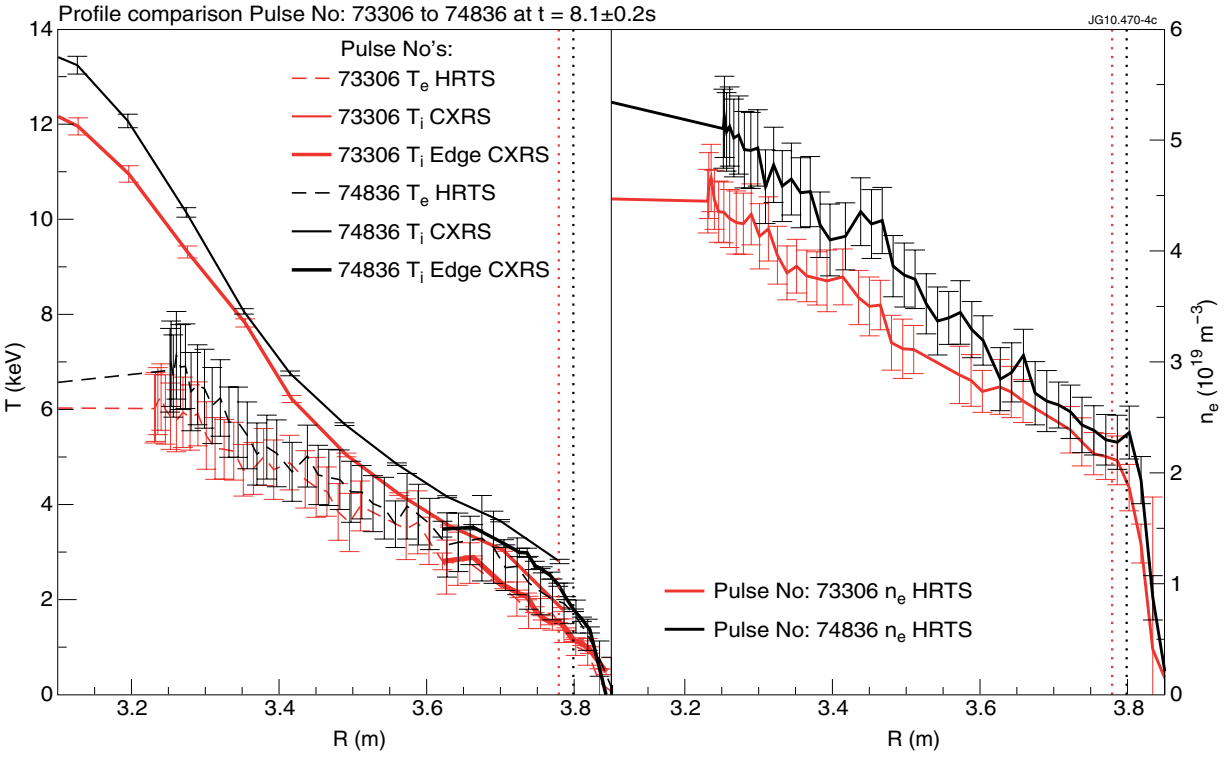

Figure 4: Temperature profiles from a pulse with modified q-profile in black (current overshoot) and without modified q-profile in red. The profile in closed lines are ion temperatures measured by Charge Exchange Recombination Spectroscopy (CXRS). Closed thick lines are from the edge CXRS system. Dashed lines are electron temperatures measured by the High Resolution Thomson Scattering (HRTS) diagnostic. On the right hand side the corresponding density profiles from HRTS. The pedestal radius used to derive the pedestal energy for table 1 is indicated as dotted line in the appropriate colour.

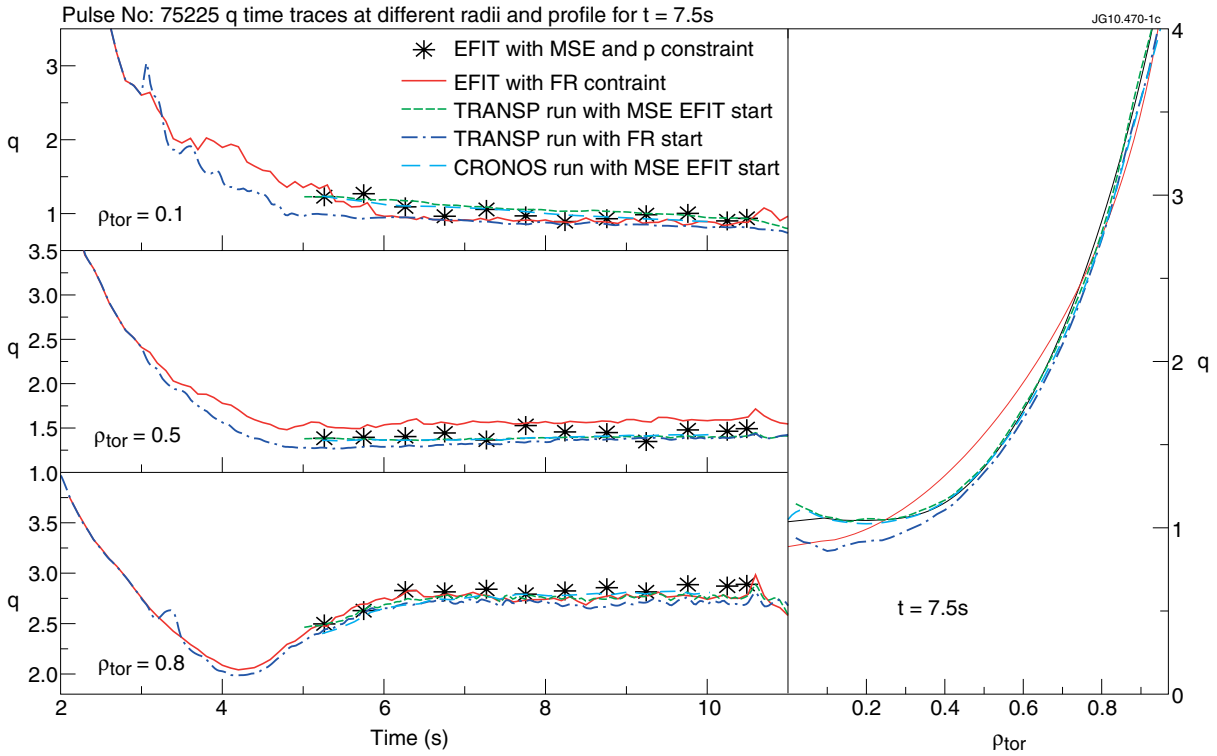

Figure 5: Time traces of q at different rtor for a low triangularity discharge.The q-profile is modified using a current ramp down. MSE and pressure constrained equilibrium in black, a Faraday rotation in a red line, an interpretative TRANSP calculation starting from a Faraday rotation q-profile at t = 3s in a dash dotted blue line, a interpretative TRANSP calculation starting from a MSE q-profile at t = 5.26s in a green dashed line and a CRONOS run starting from a MSE q-profile at t = 5.26s in a turquoise dashed line are plotted.

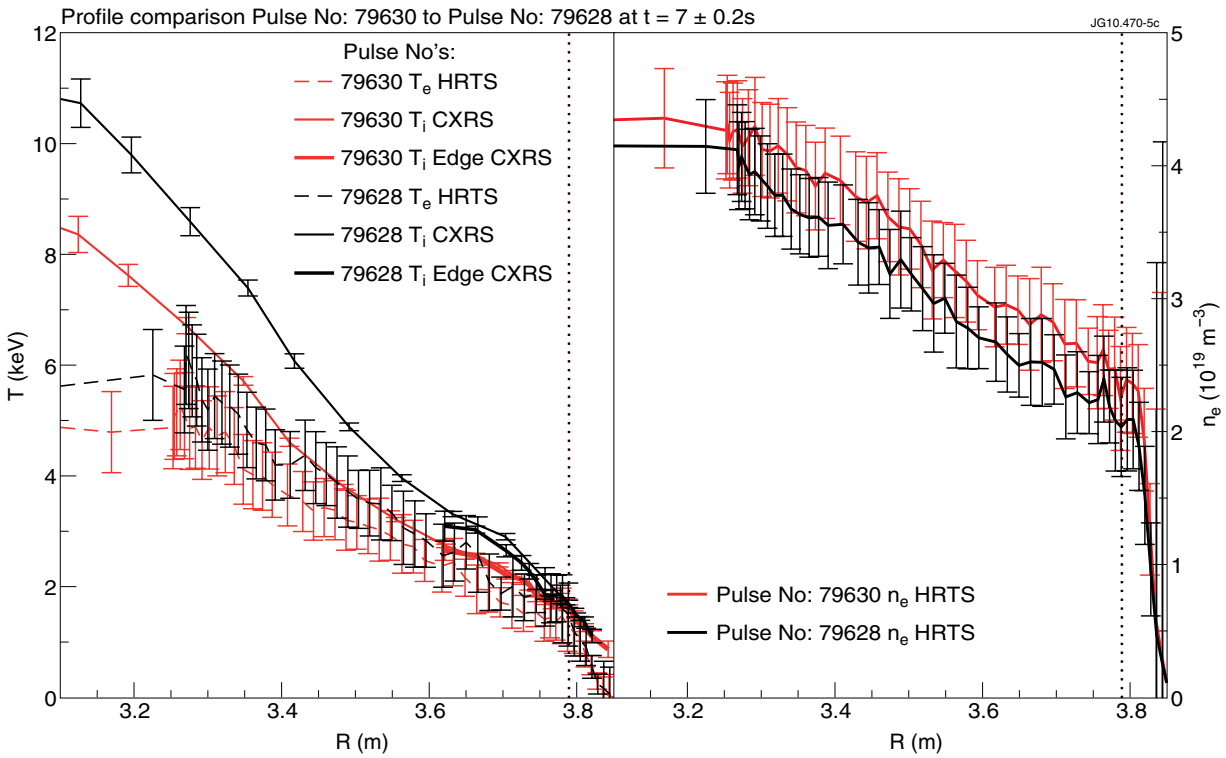

Figure 6: Temperature profiles from a pulse with modified q-profile in black (current overshoot) and without modified q-profile in red. The profile in closed lines are ion temperatures measured by Charge Exchange Recombination Spectroscopy (CXRS). Closed thick lines are from the edge CXRS system. Dashed lines are electron temperatures measured by the High Resolution Thomson Scattering (HRTS) diagnostic. On the right hand side the corresponding density profiles from HRTS. The pedestal radius used to derive the pedestal energy for table 1 is indicated as dotted line in the appropriate colour.

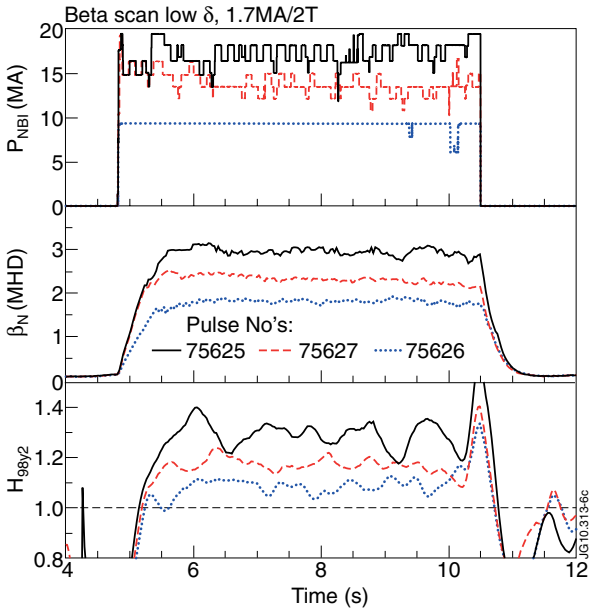

Figure 7: Time traces of three JET hybrid discharges with current overshoot in low triangularity. In the upper graph the traces of the NBI heating power are shown. In the middle the normalised beta β_N and in the lower graph the $H_{98,y2}$-factor is drawn. The $H_{98,y2}$ data is averaged over 400ms and takes the time derivative of the stored diamagnetic energy into account, this leads to a not so constant numerical value and and overestimation at the time when the NBI power is switched off.

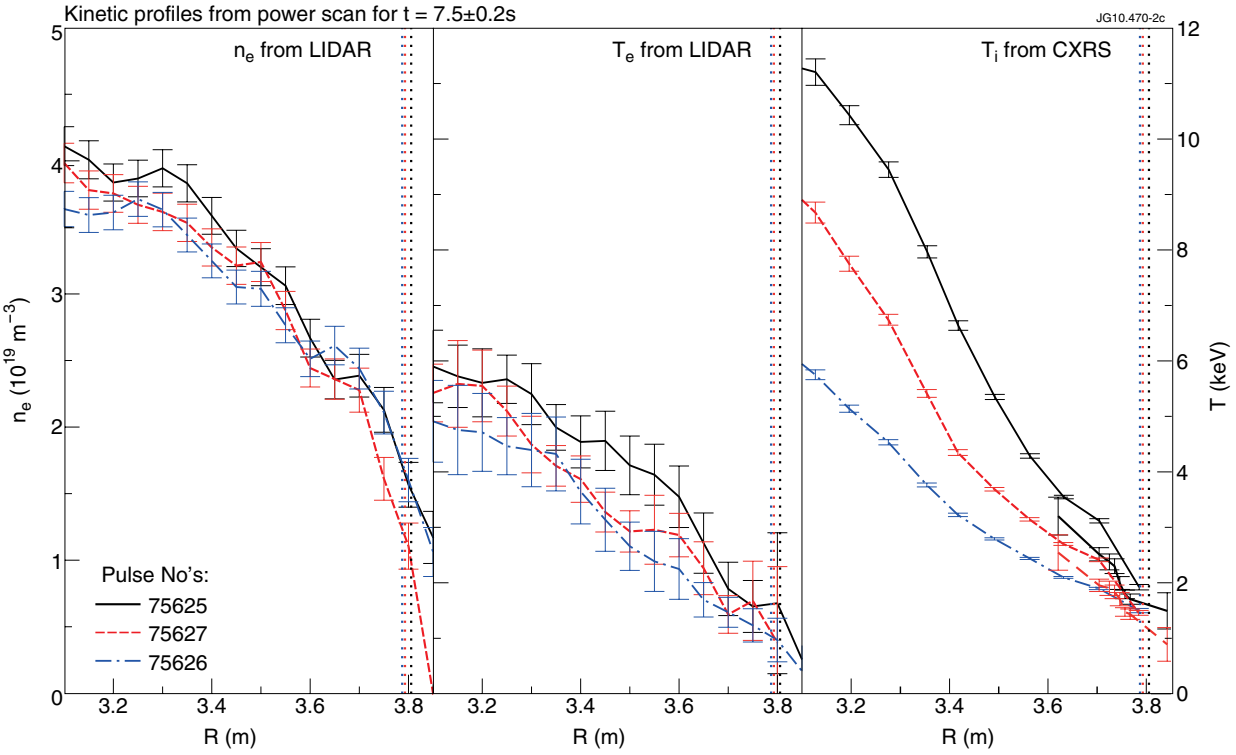

Figure 8: Kinetic profiles for the three JET hybrid discharges of figure 7 at t = 7.5s using the same colour coding. On the left side the electron density, in the middle the electron temperature and on the right the ion temperature. The temperature profiles are plotted using the same scale.The pedestal radius used to derive the pedestal energy for table 1 is indicated as dotted line in the appropriate colour.